The FEBS Journal

FEBS PRESS science publishing by scientists

Hydroxyurea-induced senescent peripheral blood mesenchymal stromal cells inhibit bystander cell proliferation of JAK2V617F-positive human erythroleukemia cells

Sunčica Bjelica[1], Miloš Diklić[1], Dragoslava Đikić[1], Marijana Kovačić[1], Tijana Subotički[1], Olivera Mitrović-Ajtić[1], Milica Radojković[2,3], Vladan P. Čokić[1] and Juan F. Santibanez[1,4]

1 Group for Molecular Oncology, Institute for Medical Research, University of Belgrade, Serbia
2 Department of Haematology, Clinical Hospital Centre Dragisa Misovic, Belgrade, Serbia
3 Faculty of Medicine, University of Belgrade, Serbia
4 Centro Integrativo de Biología y Química Aplicada (CIBQA), Universidad Bernardo O'Higgins, Santiago, Chile

Keywords
bystander effects; hydroxyurea; peripheral blood mesenchymal stem cells; proliferation; reactive oxygen species; senescence

Correspondence
J. F. Santibanez, Group for Molecular Oncology, Institute for Medical Research, University of Belgrade, Dr Subotica 4, POB 102, 11129 Belgrade, Serbia
Tel: 381 11 2685 788
E-mail: jfsantibanez@imi.bg.ac.rs

(Received 21 August 2018, revised 15 April 2019, accepted 13 May 2019)

doi:10.1111/febs.14927

Hydroxyurea (HU) is a nonalkylating antineoplastic agent used in the treatment of hematological malignancies. HU is a DNA replication stress inducer, and as such, it may induce a premature senescence-like cell phenotype; however, its repercussion on bystander cell proliferation has not been revealed so far. Our results indicate that HU strongly inhibited peripheral blood mesenchymal stromal cells (PBMSC) proliferation by cell cycle arrest in S phase, and that, consequently, PBMSC acquire senescence-related phenotypical changes. HU-treated PBMSC display increased senescence-associated β-galactosidase levels and $p16^{INK4}$ expression, as well as DNA damage response and genotoxic effects, evidenced by expression of γH2A.X and micronuclei. Moreover, HU-induced PBMSC senescence is mediated by increased reactive oxygen species (ROS) levels, as demonstrated by the inhibition of senescence markers in the presence of ROS scavenger *N*-acetylcysteine and NADPH oxidase inhibitor Apocynin. To determine the HU-induced bystander effect, we used the *JAK2V617F*-positive human erythroleukemia 92.1.7 (HEL) cells. Coculture with HU-induced senescent PBMSC (HU-S-PBMSC) strongly inhibited bystander HEL cell proliferation, and this effect is mediated by both ROS and transforming growth factor (TGF)-β expression. Besides induction of premature senescence, HU educates PBMSC toward an inhibitory phenotype of HEL cell proliferation. Finally, our study contributes to the understanding of the role of HU-induced PBMSC senescence as a potential adjuvant in hematological malignancy therapies.

Abbreviations
AAPH, 2,2′-azobis-2-methyl-propanimidamide dihydrochloride; APO, Apocynin; CFSE, 5(6)-Carboxyfluoresceindiacetate *N*-succinimidyl ester; CML, chronic myeloid leukaemia cell; DAPI, diamidine-2′-phenylindole dihydrochloride; DCFDA, 2′,7′-dichlorodihydrofluorescein diacetate; DDR, DNA damage response; H_2O_2, hydrogen peroxide; HEL, human erythroleukemia cells; HU, hydroxyurea; HU-S-PBMSC, HU-induced senescent peripheral blood mesenchymal stromal cells; IF, immunofluorescence; LAP, latency-associated peptide; MC, morphological changes; MPN, myeloproliferative neoplasms; MSC, mesenchymal stromal cells; MTT, dimethylthiazol-2-yl-2,5-diphenyltetrazolium bromide; NAC, *N*-acetylcysteine; NOX, NADPH oxidases; PBMSC, peripheral blood mesenchymal stromal cells; PB, peripheral blood; PE, phycoetrythrin; PI, propidium iodide; ROS, reactive oxygen species; RS, replicative senescence; SASP, senescence-associated secretory phenotype; SA-β-gal, senescence-associated β-galactosidase; SIPS, stress-induced premature senescence; TBRi, transforming growth factor-β type I receptor; TGF-β, transforming growth factor β.

Introduction

Hydroxyurea (HU), a well-known inhibitor of ribonucleotide reductase, is a nonalkylating antineoplastic agent used in the treatment of hematologic malignancies, infectious and skin diseases [1]. Namely, HU provokes a deoxyribonucleotides, double-strand DNA breaks near to replication forks, and inhibits both nuclear and mitochondrial DNA replication, thus causing cellular and mitochondrial dysfunctions [2]. Moreover, HU is a DNA replication stress inducer and can induce senescence-like phenotype in both transformed and primary cells [3].

Chemotherapeutic drugs can induce the persistent presence of senescent cells in normal noncancerous tissues [3,4]. *In vitro* studies have demonstrated that different transformed cell lines and primary cells, such as fibroblasts and mesenchymal stromal cells (MSC) can display a senescence-like phenotype [3]. Although MSC circulate at a very low level in healthy individuals, peripheral blood MSC (PBMSC) are increased in pathological conditions [5]. These cells are characterized by expression of CD73, CD90 and CD105, while they are negative for leukocytes differentiation markers. Also, PBMSC show the capacity to differentiate into chondrocytes, osteocytes, and adipocytes [6]. MSC as proliferating cells may undergo both replicative senescence (RS) in extended cultivation, and stress-induced premature senescence (SIPS) upon exposure to sub-cytotoxic stressors, including hydrogen peroxide (H_2O_2) and chemotherapy [3,7]. Consistent with senescence induction, cells are under a stable cell cycle arrest and complex phenotypic changes – such as cell enlargement and flattening, persistent DNA damage response (DDR), formation of heterochromatin foci, increased expression and activity of senescence-associated β-galactosidase (SA-β-gal), and senescence-associated secretory phenotype (SASP)[8,9] all occur.

One of the main mechanisms involved in both RS and SIPS is an increased oxidative stress status [3,10–12]. HU, as a stress inducer, is able to induce SIPS in a variety of transformed and primary cells, partly by increasing reactive oxygen species (ROS) level [3,13]. Nevertheless, senescent cells remain metabolically active and can interact with other cells in the tumor microenvironment by cell–cell interaction or via SASP; thus they may influence the fate of neighboring cells via paracrine effects [8,14]. However, the capacity of HU-induced senescence cells to influence bystander cells has not been well elucidated so far.

Hydroxyurea is currently used as first line of chemotherapy in malignancies, such as myeloproliferative neoplasms (MPN), which are characterized by mutation in *JAK2V617F, CALR* and *MPL* genes [15]. To test whether the induction of senescence by HU in MSC may affect bystander cell proliferation, we performed co-culture experiments with human PBMSC and the human erythroleukemia 92.1.7 cells (HEL), a representative MPN harboring *JAK2V617F* mutation. We found that HU induces premature senescence in PBMSCs, and these senescent PBMSCs have an inhibitory effect on the proliferation of co-cultured erythroleukemia cells. These results may contribute to a better understanding of how chemotherapy induced genotoxic MSC senescence affects proliferation of transformed myeloid cells.

Results

HU reduces PBMSC proliferation and induces premature senescence phenotype

In this study, we used MSC isolated from peripheral blood (PB) of healthy donors as a cell model. These cells were characterized according to the criteria proposed by Mesenchymal and Tissue Stem Cell Committee of the International Society for Cellular Therapy [16]. More than 90% PBMSC were positive for CD73, CD90, and CD105, while about 5% of the cells were positive for CD11b and CD45 (Fig. 1A). Cells also showed a fibroblastic-like phenotype when cultured in plastic surfaces (Fig. 1B). Moreover, under specific inductive media, cells differentiated into osteoblasts and adipocytes (Fig. 1C).

It has been demonstrated that HU provokes several cell responses, including cell proliferation inhibition, apoptosis and cell senescence in noncancerous cells such MSC and fibroblasts [3,17]. Here, we conducted experiments to investigate whether HU can influence PBMSC proliferation and induce cell changes related to genotoxic senescence. HU induced inhibition of cell proliferation after 3 and 6 days of treatment with increasing concentrations of the drug, as determined by the MTT assay (Fig. 2A). At 3 days treatment 100 μM of HU induced an inhibition in about 25%, and reached about 33% of inhibition upon higher HU concentrations up to 600 μM. Similarly, 6 days treatment induces 37% and 42% of cell growth inhibition.

The effects on cell proliferation were in concordance with changes in cell cycle at 3 days treatment, as HU (200 and 400 μM) induced cell cycle arrest in S phase at the detriment of cells in G_0/G_1 and G_2/M cell cycle phases (Fig. 2B,C). Moreover, PBMSC treated for 6 days with 200 μM HU showed similar increased S phase frequency and reduced G_0/G_1 and G_2/M cell cycle phases.

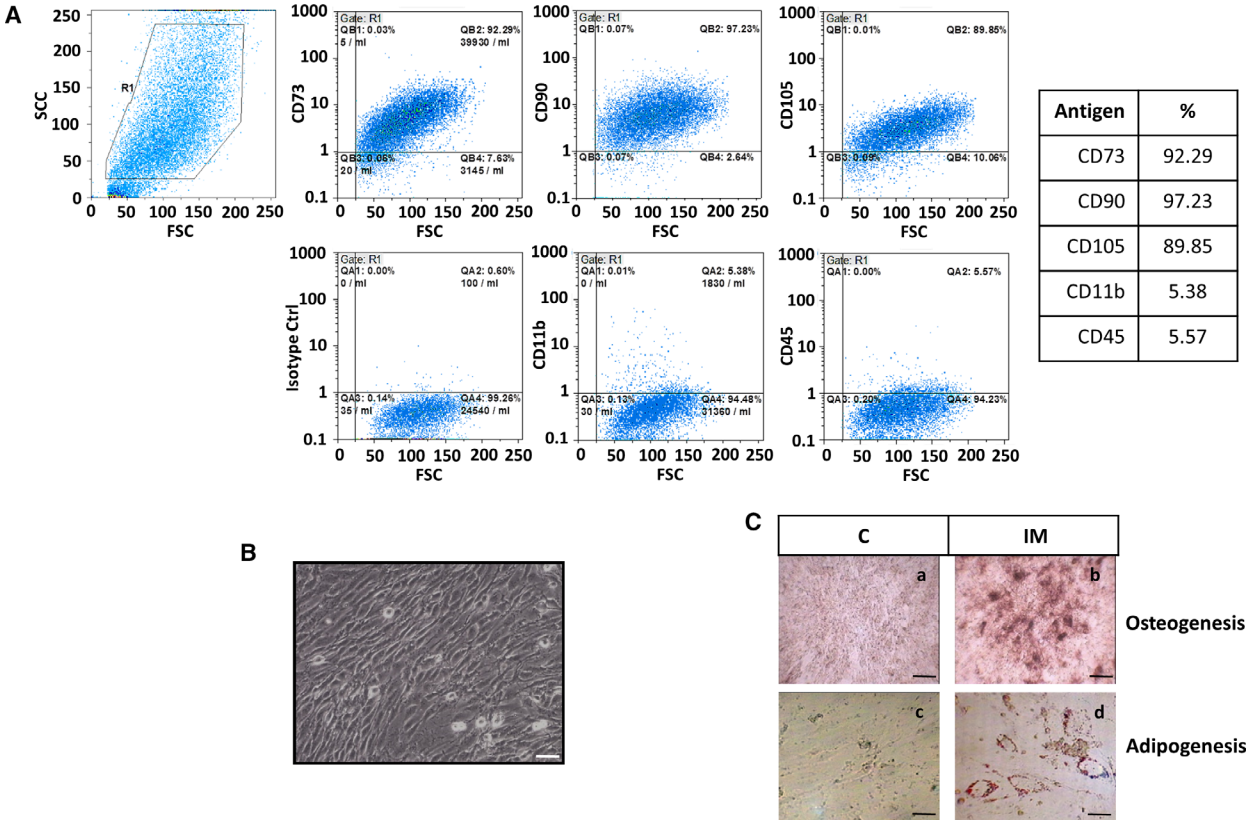

Antigen	%
CD73	92.29
CD90	97.23
CD105	89.85
CD11b	5.38
CD45	5.57

Fig. 1. PBMSC characterization. (A) PBMSC immunophenotyping. Isolated PBMSC were subjected to (CD73, CD90 and CD105) and leukocyte cell surface markers (CD11b and CD45). (B) PBMSC morphology. Cells were photographed at third passage by using inverted microscopy. (C) PBMSC osteogenic and adipogenic differentiation potential. Cells were treated with indicated induction media and stained for mineralization content or lipid droplet accumulation for the respective osteogenic and adipogenic differentiation.

Next, we performed experiments to determine whether cell proliferation inhibition associated with HU in PBMSCs was associated with cellular senescence. HU provoked profound PBMSC morphological changes (MC): they became enlarged, irregularly shaped and flattened which was noticed on the third and the sixth day of treatment (Fig. 3). Also, SA-β-gal expressed cells were mostly noticeable after 3 days of treatment and there number was increased 6 days upon HU challenge (Fig. 3A,B). Moreover, the cyclin-dependent kinase inhibitor $p16^{INK4}$ expression was apparent 24 h after applying HU and was maintained throughout the entire HU treatment period. Another cyclin-dependent kinase inhibitor, p21, was weakly induced from the day three of drug treatment. Moreover, cells that were treated with HU for 3 days and cultivated without treatment for three more days (3 + 3) expressed SA-β-gal and $p16^{INK4}$ similarly to the level observed on the day three of HU treatment. Thus, the results suggested that in our experimental conditions HU induced a PBMSC premature senescence phenotype in an irreversible way.

Persistent DNA damage induced by HU treatment

Next, to explore whether HU-induced senescence may implicate genotoxic mechanisms, γH2AX foci expression, as a marker of DNA double strand breaks, was analyzed. However, 3 and 6 days of HU treatment induced the expression of nuclear γH2A.X, which was absent in control cells (Fig. 4A,B). Furthermore, micronuclei localized next to the enlarged nuclei were generated after 3 and 6 days of HU treatment (Fig. 4C). Thus, these data suggest that HU may induce persistent genotoxic effects on PBMSC.

HU increases reactive oxygen species levels to induce PBMSC senescence-like phenotype

Cell senescence is frequently accompanied by increased intracellular ROS level [12]. Consequently, we addressed experimental assays to determine whether HU operates via oxidative stress mechanisms. Figure 5A shows that increased HU dose induced higher

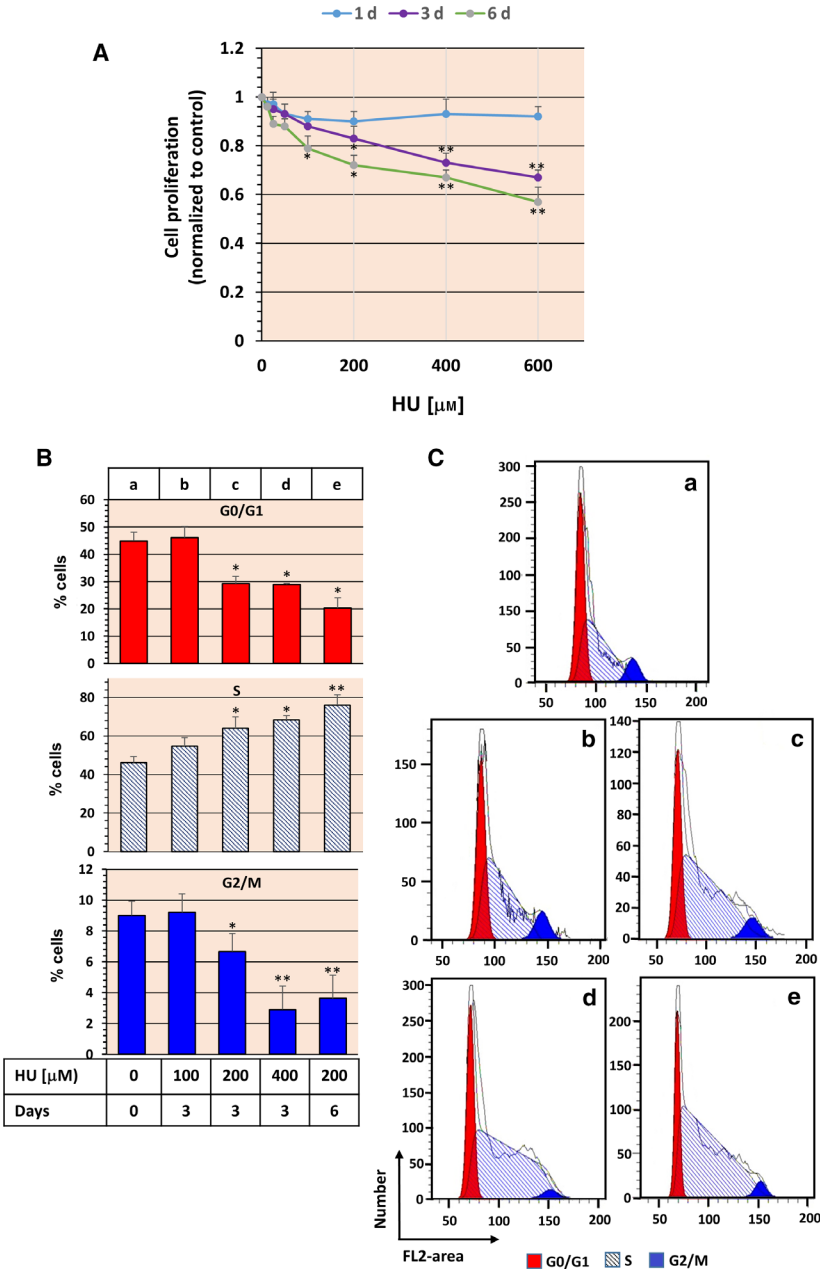

Fig. 2. HU inhibits PBMSC proliferation. (A) MTT analysis of PBMSC treated with increased HU amounts for 1 day (d), 3 days and 6 days, blue, violet, and green lines, respectively. (B, C) Cell cycle analysis by PI staining. Cells were treated for 3 days with HU at indicated concentrations and for 6 days with 200 mM HU. Bar graph of % of cell cycle phase distribution indicated that HU at 200 and 400 μM mainly reduces G_0/G_1 cell frequency while increases cell percentage in S phase. Histograms of events by DNA content show cell cycle distribution, a, b, c, d, and e represent experimental conditions indicated in graphic bar. Representative results as means ± SEM from three independent determinations are shown. Significant difference from the control condition by *t*-test: $*P < 0.05$ and 0.005 (**).

ROS levels in comparison to untreated cells. Moreover, 200 μM HU provoked a threefold ROS levels increase after 1 day of treatment, which was maintained through the next days (Fig. 5B). In order to determine whether ROS contribute to HU-induced senescence, we challenged PBMSCs with HU for 3 days in presence of Apocynin (APO), an inhibitor of NADPH oxidases (NOXs) [18] and *N*-acetylcysteine (NAC), a ROS scavenger [19]. The presence of APO or NAC inhibited the expression of SA-β-gal and $P16^{INK4}$ induced by HU (Fig. 5C,D) indicating that ROS-mediated HU-induced senescence. Due to the fact that some NOXs (Nox1-3) are Rac1 dependent [20], we treated cells with Rac1 inhibitor NSC23766. The presence of this inhibitor did not influence the capacity of HU to induce SA-β-gal and p16 expression (Fig. 5C), suggesting that NOXs Rac1-dependent enzymes are not implicated.

Further, we performed experiments to determine the role of oxidative stress in HU-inhibited PBMSC proliferation. MTT assay demonstrated that APO and NAC were protecting cells from cell proliferation inhibition

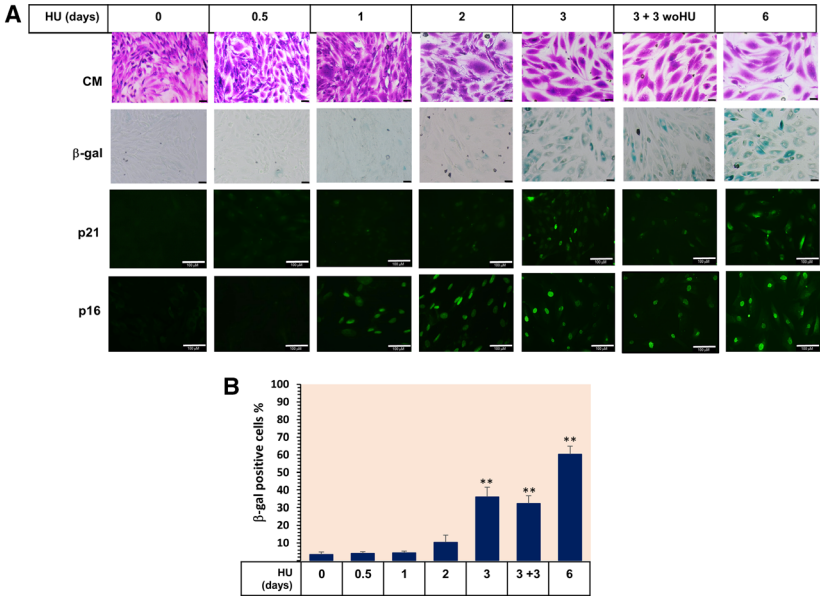

Fig. 3. HU induces a PBMSC senescence-like phenotype. (A) PBMSC were treated for the indicated days with 200 μM of HU and subjected to MC analysis by crystal violet staining (first row), β-galactosidase activity by histochemistry assay (second row). Magnification 20×, scale bars 50 μm. IF analysis of $p21^{CIF1}$ (third row) or $p16^{INK4}$ (fourth row), magnification 20× and scale bars 100 μm. (B) Graph indicates senescent cell counts at the indicated periods of treatment. The results are representative of three replicates as means ± SEM. $^{**}P < 0.005$ vs. untreated cells.

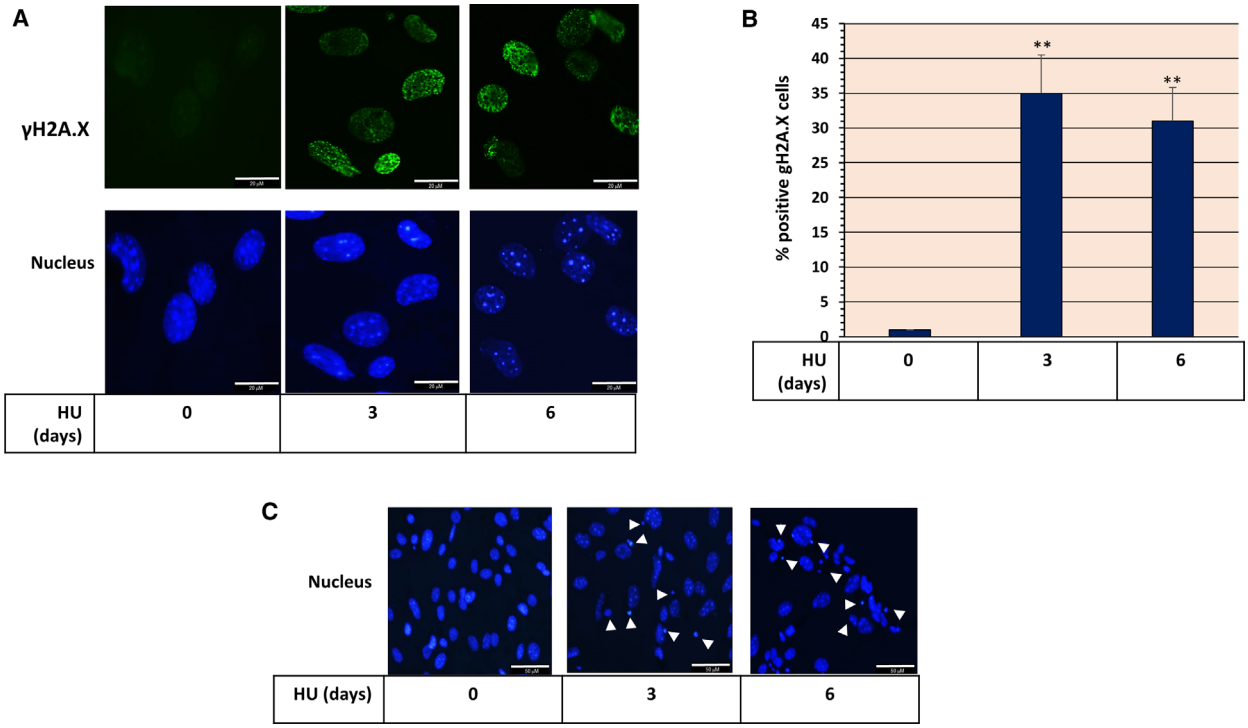

Fig. 4. HU induces PBMSC genotoxicity. (A) HU induced formation of DNA double-strand breaks in PBMSC. IF analysis for γH2AX (green) in cells treated for 3 and 6 days with HU at 200 μM. The formation of γH2AX foci (green) represents the biochemical marker of DNA double-strand breaks. Cells were counterstaining with DAPI to detect cell nuclei (blue). Magnification 100×, scale bars 20 μm. (B) Graph indicates γH2AX positive cells percentage the indicated periods of treatment. The results are representative of three replicates as means ± SEM. $^{**}P < 0.005$ vs. untreated cells. (C) Determination of micro-nuclei formation in HU-treated PBMSC. Cells were treated as in (A) fixed and DAPI stained. Micronuclei are indicated with white arrows. Magnification 40×, scale bars 50 μm. Representative results from three independent determinations are shown.

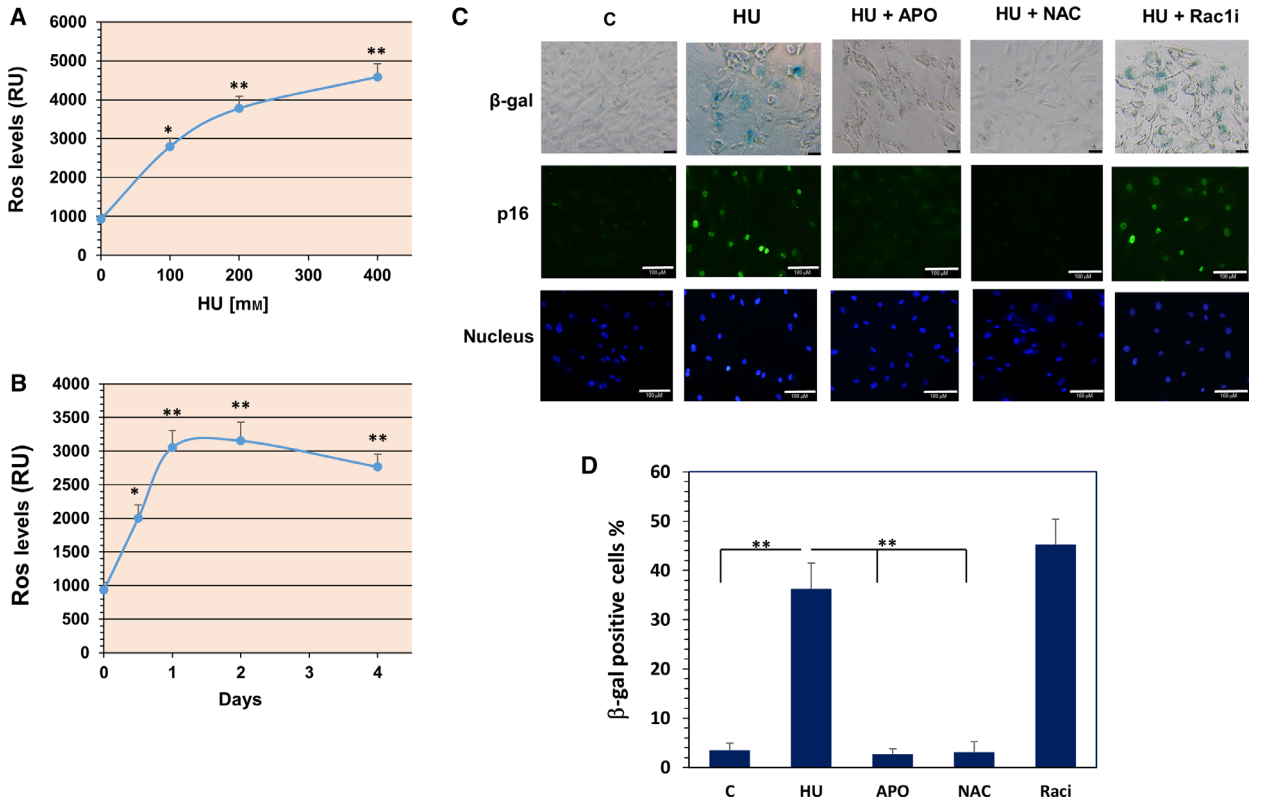

Fig. 5. ROS mediates HU-induced PBMSC senescence-like phenotype. (A) PBMSC were treated for 3 days with increased HU concentrations. At the end of incubation time, cells were loaded with DCFDA and intracellular florescence was analyzed to determine ROS levels. Significant difference from the control condition by *t*-test: $*P < 0.05$ and 0.005 (**) (B) Cells were treated during 4 days with 200 μM HU and intracellular ROS levels was determined. The results are representative of three replicates as means ± SEM. $*P < 0.05$ and $**P < 0.005$, vs. untreated cells. (C) Cells were treated for 3 days with 200 μM HU in the presence of 100 μM APO, 5 mM NAC or 25 μM with Rac1 inhibitor NSC23766 trihydrochloride (Rac1i) and subjected to senescence analysis. The presence of APO or NAC prevented HU induction of β-gal (upper photographs) and $P16^{INK4}$ expression (middle photographs) determined by immunocytochemistry (magnification bars 40 μM) or IF (magnification bars 100 μM) assays respectively. IF assayed cells were counterstained with DAPI to detect cell nuclei (bottom photographs). Representative results from at least three independent determinations are shown. (D) Graph indicates senescent cell counts at the indicated treatments. The results are representative of three replicates as means ± SEM. $**P < 0.005$ vs. untreated cells.

by 200 μM of HU, while APO or NAC alone did not significantly modify basal PBMSC proliferation (Fig. 6A). Cell cycle analyses showed that APO and NAC in co-treatment with HU, mainly restored G_0/G_1 frequency to the control levels, while S phase proportion was reduced (Fig. 6B,C). Together, these data suggest that ROS levels mediate HU induction of PBMSC senescence and inhibition of proliferation.

HU-induced senescence PBMSCs proliferation inhibition of bystander HEL cells

Mesenchymal stromal cells have been implicated both in inhibition and support of cell growth [21,22], while HU is the first line of therapy for MPN [1]. We were wondering whether HU-induced genotoxic senescence might regulate the capacity of MSC to support proliferation of HEL cells, a HEL line harboring *JAK2V617F* mutation. Accordingly, HU-induced senescent PBMSC (HU-S-PBMSC) were co-cultivated with 5(6)-Carboxyfluoresceindiacetate *N*-succinimidyl ester (CFSE) labeled HEL cells, as bystander cells, and incubated for 3 days. CFSE-staining HEL cells were mytomycin treated to block cell proliferation at the beginning of experiments and named as zero time cells, these cells representing full CFSE-stained cells. HEL cells, co-cultured with 200 μM HU pretreated PBMC for either 3 or 6 days, showed inhibited proliferation activity as is demonstrated by reduced proliferation index (Fig. 7A) and CFSE dilution capacities (Fig. 7B). Moreover, there were no significant difference in the effect on HEL cell proliferation inhibition between 3 and 6 days pretreated PBMSC. Furthermore, the same capacity of 3 and 6 days HU

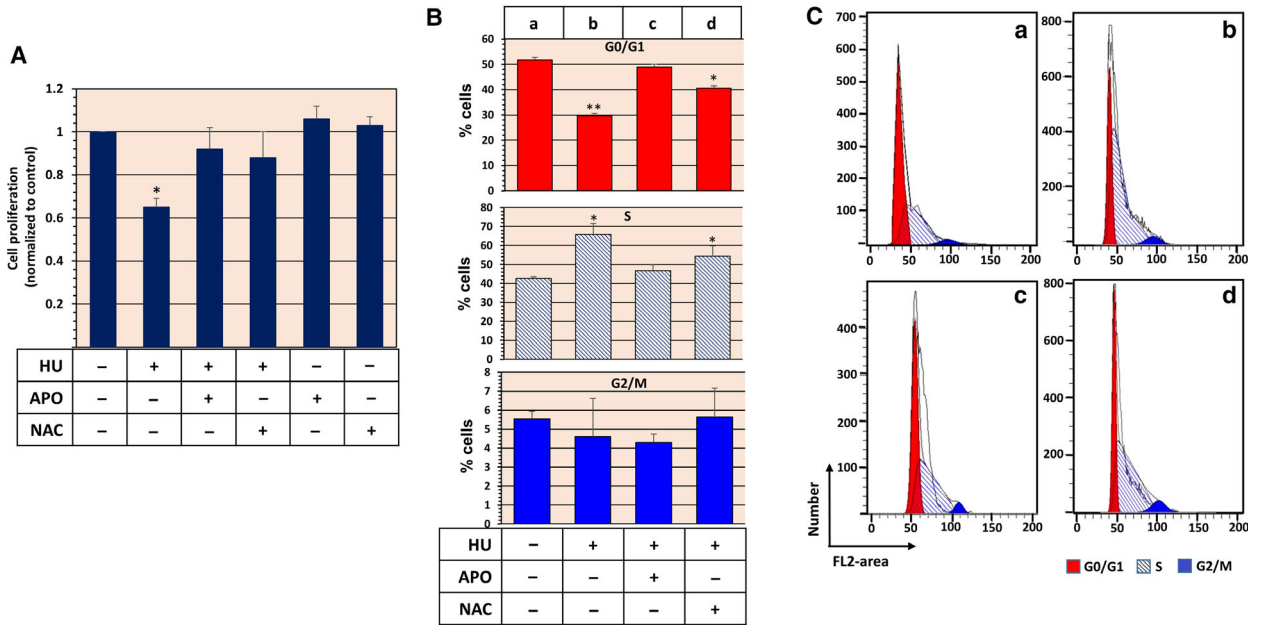

Fig. 6. ROS mediates HU-inhibited PBMSC proliferation. (A) MTT assay of PBMSC treated with HU in presence or absence of APO or NAC for 3 days. Representative results as means ± SEM from three independent determinations are shown. Significant difference from the control condition by *t*-test: $*P < 0.05$. (B, C) NAC and APO protected PBMSC accumulation in cell cycle S phase induced by treatment with 200 μM of HU. Cells were treated for 3 days with HU and APO or NAC and subjected to cell cycle analysis by PI stained. Bar graph of percentage of cell cycle phase distribution is shown (left figure). Histograms representing cell cycle distributions (right figure), a, b, c, and d represent experimental conditions indicated in graphic. Representative results as means ± SEM from at least three independent determinations are shown. Significant difference from the control condition by *t*-test: $*P < 0.05$ and $**P < 0.005$.

pretreated PBMSC to inhibit HEL cell proliferation was confirmed by MTT assay (Fig. 7C).

ROS and transforming growth factor-beta1 mediate HU-S-PBMSC inhibition of HEL cell proliferation

We also tested two potential mechanisms by which the senescent PBMSCs could mediate the changes in bystander cell proliferation: ROS and the Transforming Growth Factor-beta1 (TGF-β1) pathways that have been considered as a part of SASPs among others factors [23]. Figure 8A,B shown HEL cell sensitivity to H_2O_2 or 2,2′-azobis-2-methyl-propanimidamide dihydrochloride (AAPH) [24], which may indicate that HU-S-PBMSC elevated ROS levels affected cell proliferation. Furthermore, HU treatment induced TGF-β1 gene and soluble TGF-β1 expressions that is strongly blocked by APO (Fig. 8C,D) and determined by PCR and ELISA analysis, while TGF-β1 treatment reduced HEL cell proliferation (Fig. 8E). Afterwards, HEL cells were treated with APO (100 μM), to inhibit ROS production, or 4 $\mu g \cdot mL^{-1}$ latency-associated peptide (LAP) or 0.1 μM SB525334 [a selective inhibitor of transforming growth factor-β type I receptor (TBRi)] to reduce TGF−β1 bioavailability and inhibit TGF-β type I receptor activity respectively. The selected concentration of inhibitors did not affect HEL cell proliferation (Fig. 8F).

Next, we performed co-culture experiments to determine whether ROS and/or TGF-β1 were implicated in the capacity of HU-S-PBMSC to reduce HEL cell proliferation. Since no significant differences were found between 3 and 6 days of PBMSC treatment on HEL cell proliferation, we performed the next assays using 3 days HU-treated PBMSC. As shown in Fig. 9A,B, co-culture assays indicated that control PBMSC did not affect HEL cell growth compared with HEL cells growing alone, as demonstrated by proliferation index and CFSE dilution assay. Meanwhile, HU-S-PBMSC provoked a significant reduction in proliferation index and CFSE dilution, while either the presence of APO, LAP or SB525334 protected bystander HEL cells from HU-S-PBMSC inhibition.

The inhibition of HEL cell proliferation was further confirmed by cell cycle analysis. HEL cells co-cultured with HU-S-PBMSC showed an increase of cell frequency at G_0/G_1 phase to the detriment of mainly S cell cycle phase, while HEL cells co-cultured with untreated PBMSC, or with HU-S-PBMSC in presence

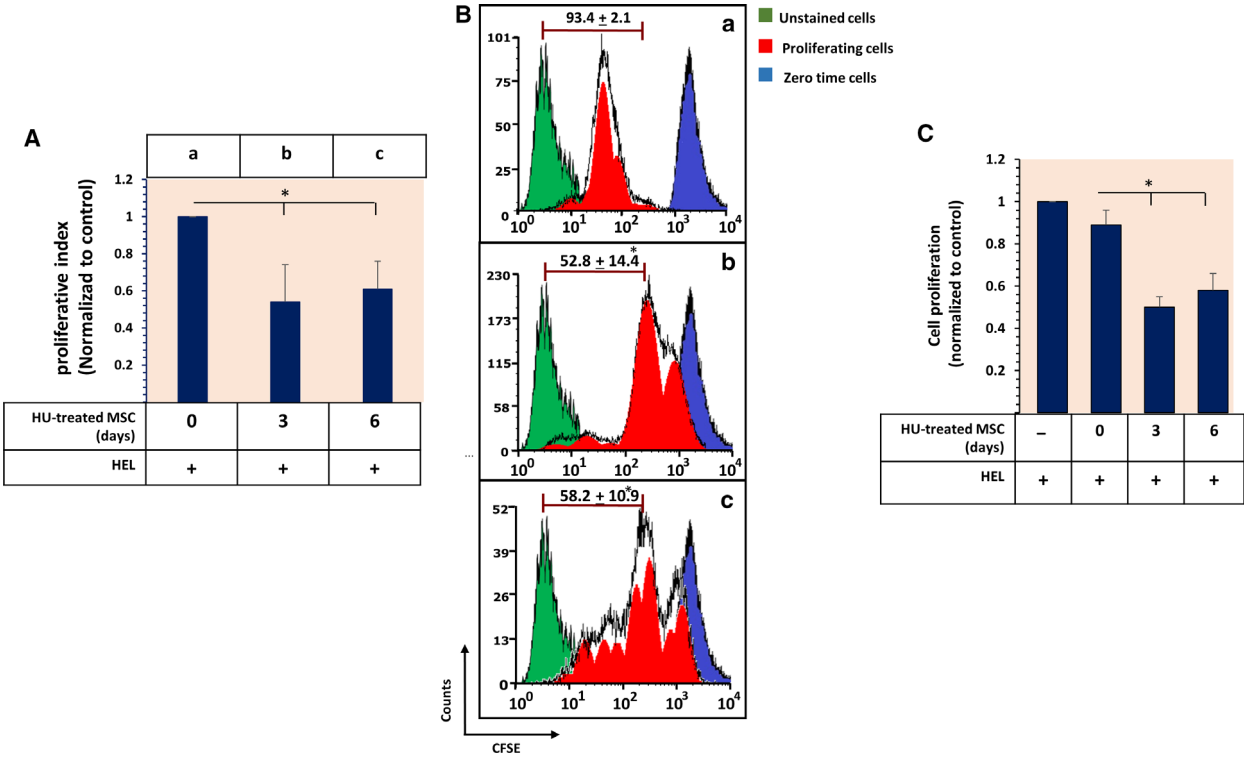

Fig. 7. HU-S-PBMSC inhibits HEL cell proliferation in co-culture conditions. (A) The bars plot represent proliferative index of CFSE-stained HEL cells co-cultured for 3 days with HU-treated PBMSC as is indicated. (B) Histogram of HEL cells CFSE stained and co-cultured with PBMSC as in A. Brown bars represent the percentage of cells at the indicated area as results of CFSE dilution. HEL cells just after CFSE staining were treated for 30 min with mytomycin C (40 $\mu g \cdot mL^{-1}$) and named as zero time cells. a, b, and C represent experimental conditions indicated in graphic A (top). (C) MTT analysis of HEL cell proliferation co-cultured with PBMSC pre-treated HU at the indicated periods. Representative results as means ± SEM from three independent determinations are shown. Significant difference from the control condition by *t*-test: $*P < 0.05$.

of either APO or LAP, displayed similar cell cycle distribution to HEL cells alone (Fig. 10A,B). Although, HEL cells co-cultivated with HU-S-PMSC seemed to display reduced G_2/M cell cycle frequency, these differences were not statistically significant. Thus, these results suggest that, in co-cultured conditions, increased ROS and TGF-β1 levels mediate the capacity of HU-S-PBMSC to inhibit HEL cell proliferation.

Discussion

In this study, we analyzed the capacity of HU to induce premature senescence in PBMSC, and how these senescent PBMSC affect proliferation of erythroleukemia cells harboring *JAK2V617F* mutation. We determined that HU inhibits PBMSC proliferation accordingly to MTT and cell cycle analyses. Mainly HU treatments caused increased S phase frequency at detriment of G_0/G_1 phase. HU inhibits proliferation in several organisms and cell lines, mainly by arresting proliferating cells in the S cell cycle phase due to the decrease of dNTPs levels. HU limits the cellular supply of deoxyribonucleotides by acting as an inhibitor of ribonucleotide reductase [17], which reduces DNA polymerase movements at replication forks, and acts as a replication stress inducer [1,3]. HU seems to allow cells entry into early steps of S phase, decelerate S phase progression and pause before mitosis [25], without affecting cell progress from G_1 to S phase [26], which can explain the increment of S phase frequency and reduction in G_0/G_1 phase. Beside G_0/G_1 effects, a reduction of G_2/M cell proportion were found. Although we have no explanation, it is possible to speculate that in these conditions, the cell remained in G_2/M, independently of S phase accumulation, progressed in cell cycle, but when they enter in a new duplication round, in the presence of HU, they were accumulated in the S phase and did not progress to G_2/M. Nevertheless, further experiments are necessary to elucidate G_2/M cell cycle phase reduction.

Hydroxyurea is frequently used as an antitumor agent because its cytoreduction effects [27], while oral

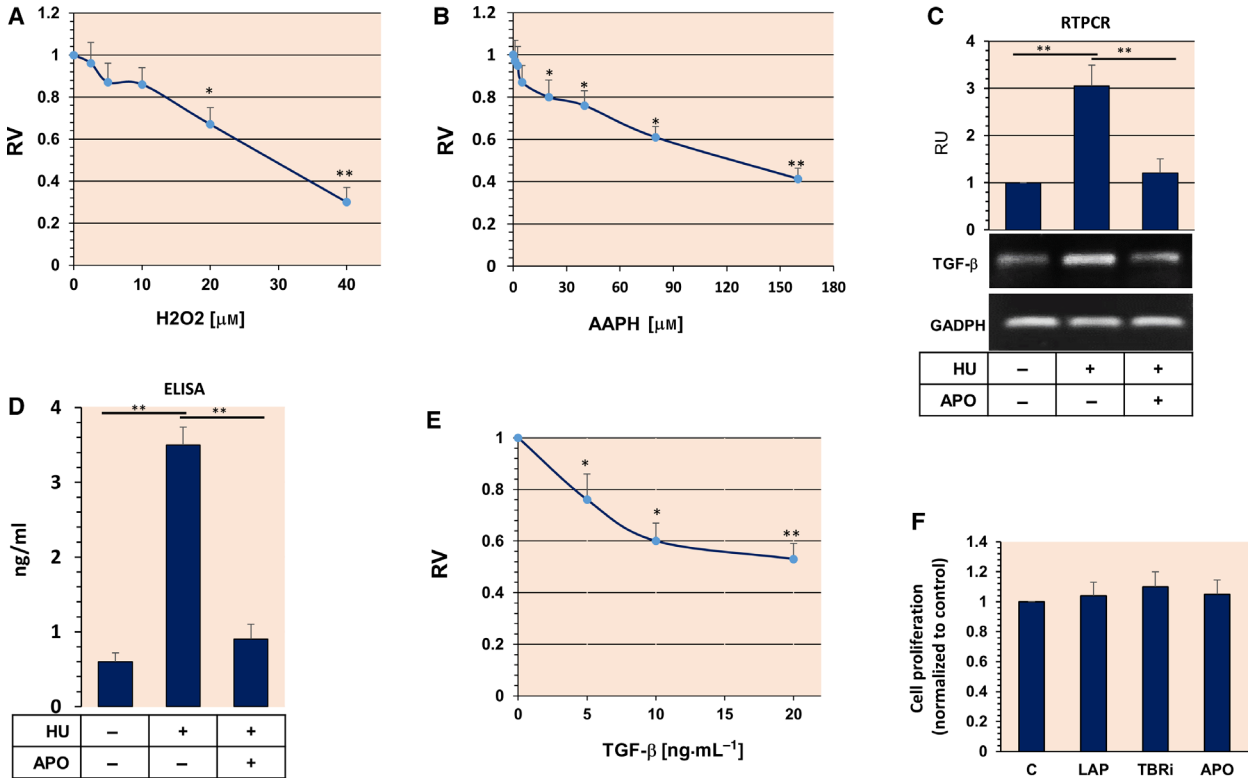

Fig. 8. ROS and TGF-β1 inhibit HEL cells proliferation. (A) HEL cells were treated for 3 days with increasing concentrations of H_2O_2 and subjected to MTT analysis. (B) HEL cells were treated for 3 days with increased amounts of AAPH (a water-soluble radical generator) subjected to MTT analysis. (C, D) HU increase TGF-β mRNA and protein expression/secretion by ROS induction. PBMSC cells were treated for 3 days with 200 μM of HU in presence or absence of 100 μM APO and subjected to RTPCR and ELISA analyses. GAPDH was used as housekeeper gene. Bands were analyzed by densitometry and semiquantitative analysis of TGF-β1/GADPH is shown as bar plot. RU, relative units. Significant difference from the control (untreated cells) by *t*-test: $*P < 0.05$ and $**P < 0.005$. Bars represent means ± SEM. (E) TGF-β1 inhibits HEL cells proliferation. Cells were treated for 3 days with increasing TGF-β concentrations and subjected to MTT analysis. Representative results as means ± SEM from three independent determinations are shown. (F) MMT assay for LAP, TBRi and APO 3 days treatment of HEL cells. Bars represent means ± SEM. Significant difference from the control (untreated cells) by *t*-test: $*P < 0.05$ and $**P < 0.005$.

HU regimen results in the average plasma HU concentrations are in 100–200 μM range [28]. This corresponds to a concentration range used in this study, which allowed us to work *in vitro* using physiologically relevant HU concentrations. Our results indicate that HU-induced senescence-like phenotype in PBMSC, with changes in cell morphology and increased SA-β-gal and $p16^{INK4A}$ expressions. Also, HU moderately increased $p21^{Cip1}$ expression. Intriguingly, it has been suggested that HU-induced S-phase arrest that seems to be independent of p53 and lower in response to the p53 target gene $P21^{Cip1}$ [26,29]. This is similar to our observations, were $p21^{Cip1}$ expression is not the main response to HU compared to the $p16^{INK4A}$ expression [30]. Moreover, it was reported that the relative $p21^{Cip1}$ unresponsiveness may provoke S phase arrest in response to DNA damage [31].

One of the consequences caused by DNA synthesis inhibition is DNA damage such as strand breaks, which is consistent with the capacity of HU, as a replication stress inducer, to generate DDR [3]. HU treatment of PBMSC increased the expression of γH2AX and the presence of micronuclei, which indicates the capacity of HU to activate DDR and its genotoxic effects [8]. It has been suggested that HU reversibly affects DNA replication, which identified this drug as a cytostatic agent; however, it may provoke low level of DNA damage by inhibiting DNA repair, without significant RNA and protein synthesis influence [1,17].

To understand the underlying mechanisms involved in the HU induction of PBMSC senescence, we analyzed the influence of HU on oxidative stress. ROS-mediated oxidative stress has been implicated in the etiology of premature cellular senescence of MSC

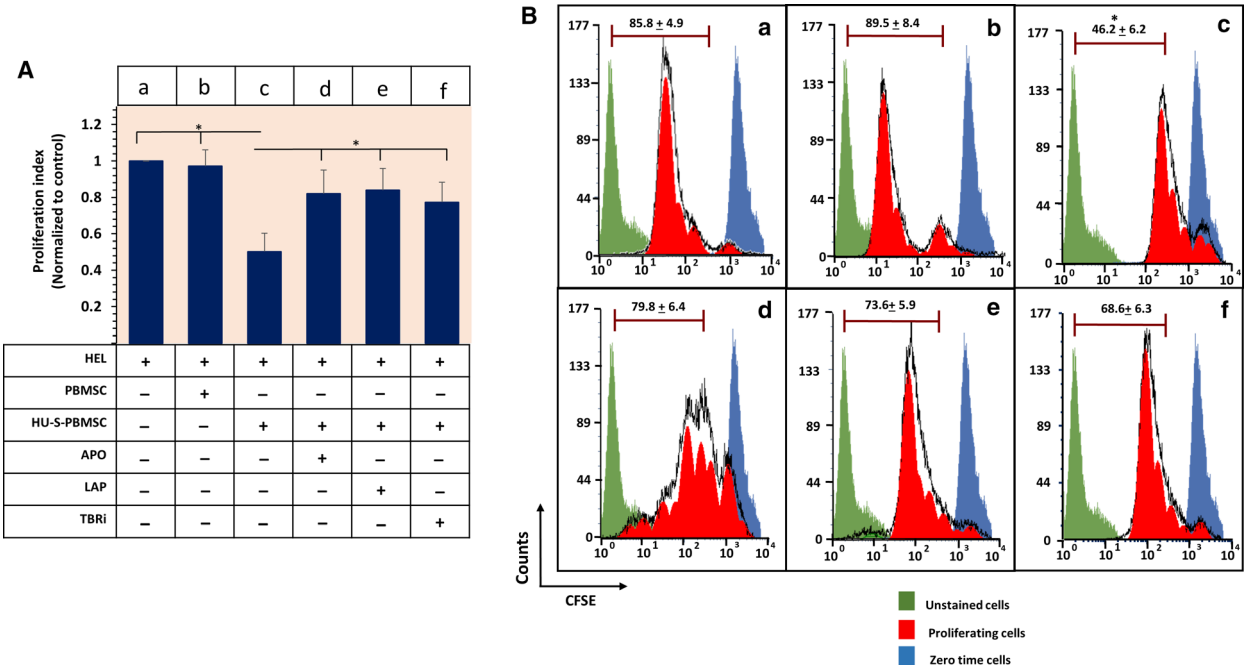

Fig. 9. HU induction of oxidative stress and TGF-β1 contributes to inhibition of HEL cell proliferation by HU-S-PBMSC. (A) Plot represent proliferative index of CFSE-stained HEL cells co-cultured for 3 days with 3 days HU-pretreated PBMSC in presence or absence of APO, to inhibit ROS production, or LAP to reduce TGF-β1 bioviability or TBRi. Bars represent means ± SEM. Significant difference control cells by *t*-test: $*P < 0.05$ (B) Histogram of HEL cells CFSE stained and co-cultured with PBMSC as in A. Brown bars represent the percentage of cells at the indicated area as results of CFSE dilution. a, b, c, d, e and f represent experimental conditions indicated in graphic A. Brown bars represent the percentage of cells at the indicated area as results of CFSE dilution. Representative results as means ± SEM from three independent determinations are shown. Significant difference from the control condition by *t*-test: $*P < 0.05$.

[10,11,32]. HU treatment induced elevated ROS levels in PBMSC and the use of inhibitors of ROS expression and ROS scavengers protected PBMSC of HU-dependant senescence induction. Furthermore, anti-oxidative stress agents protected cells from the increased cell cycle S phase frequency and inhibition of cell proliferation induced by HU.

The capacity of HU to increase ROS levels is not well elucidated yet, but some studies revealed that HU could cause DNA damage at thymidine and cytosine residues via increasing H_2O_2 [13]. Moreover, HU through induction of fork collapse may induce ROS levels [1]. Nevertheless, these findings have been observed in yeast and bacteria and it is necessary to validate this HU effect in mammalian cells [33]. On the other hand, HU induces H_2O_2 in V79 Chinese hamster cells. Our findings, by using APO, allow us to implicate NOXs as mediators of HU-induced ROS [34]. Furthermore, we included in our experiments a Rac1 inhibitor, which did not affect the induction of senescence-like phenotype of PBMSC under HU treatment. Three types of NOXs are Rac1 dependent, Nox1-3 [35], which suggests that a Rac1-independet NOX, such Nox4, may mediate HU increased ROS levels. In addition, APO protects MSC from H_2O_2 senescence induction and bone differentiation [36], which suggested APO as an antiaging agent by controlling ROS cellular production. Furthermore, Yu *et al.* [37] reported that ROS may accelerate the G1-S phase transition, so it is possible to speculate that the increased ROS levels observed in PBMSC treated with HU hasten G_1-S transition, meanwhile HU reduces the cell S exit to G_2/M, thus increasing S phase frequency.

Noticeably, HU induces senescence-like phenotype in several types of cells including transformed erythroleukemia cells, neuroblastoma, and hepatoma cells [38–40] and primary cells such human fibroblast and human dental follicle stem cells [41,42], and in human PBMSC (this study). However, the influence of senescence MSC on other cells in the tumor microenvironment or circulating transformed cells has not been established yet. Despite the senescence induction, growth arrested cells remain metabolically active and they can communicate with the microenvironment through a circuit of SASPs. SASPs comprise an array

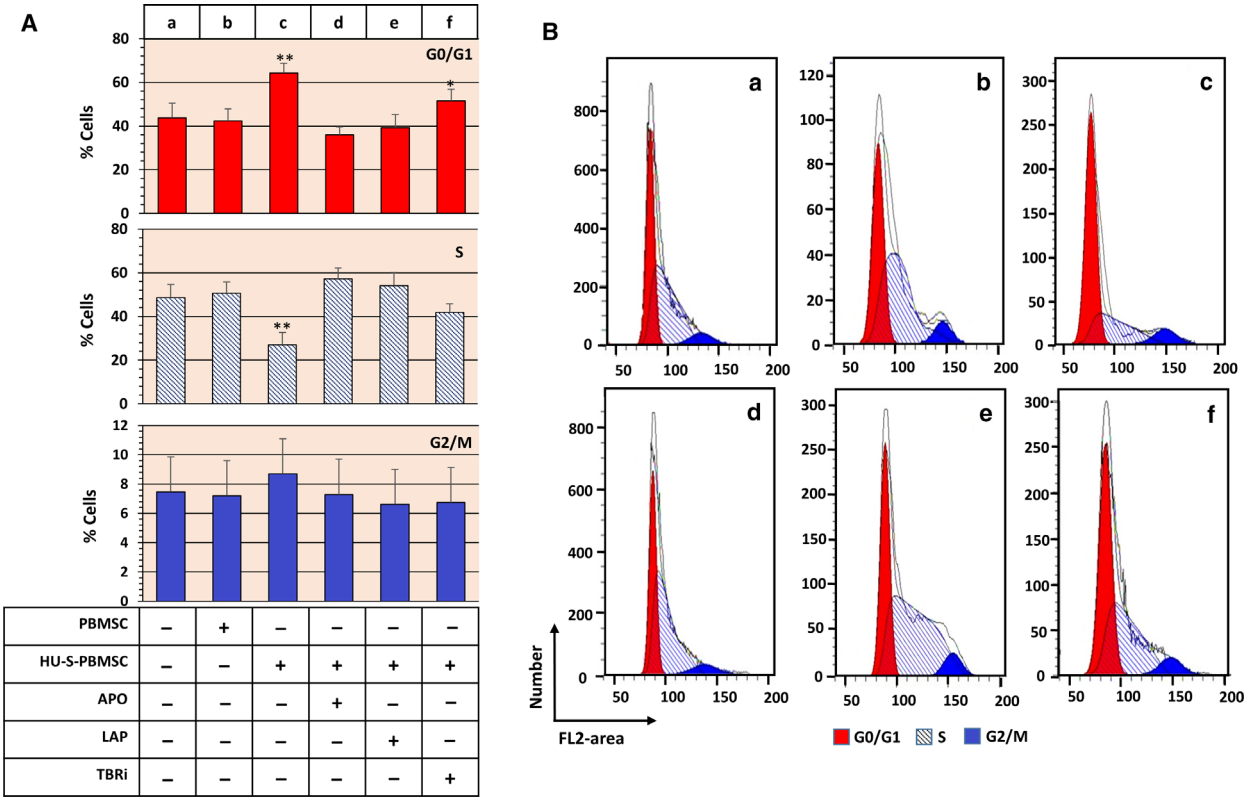

Fig. 10. ROS and TGF-β1 receptor inhibition protect HEL cells from inhibition of proliferation by HU-S-PBMSC. (A) APO, LAP and TBRi protected CFSE-stained HEL cells from HU-S-PBMSC inhibition of cell proliferation in co-culture conditions. Plot bar represent percentage of cell cycle distribution. Bars represent means ± SEM. Significant difference control cells by *t*-test: $*P < 0.05$ and $**P < 0.005$. (B) Cell cycle distribution histograms of gated CFSE-stained HEL cells analyzed for cell cycle determination after PI stain are shown. a, b, c, d, e, and f represent experimental conditions indicated in graphic A. Representative results from three independent determinations are shown.

of soluble factors with diverse biological activities, which may influence the fate of neighboring cells via bystander effects [8,14]. These paracrine effects include growth inhibition and DNA damage induction, which can be a result of SASPs expression of such as TNF-α, nitric oxide, ROS, and TGF-β1, among others [43].

Since HU is used as a well-tolerated anti-proliferative agent in the treatment of MPN [1], we selected the HEL cell line as bystander cells, which is a representative MPN cell line defined by the *JAK2V617F* mutation [44]. HEL cell proliferation is inhibited by oxidative stress of HU-S-PBMSC. Furthermore, HU increased PBMSC expression of TGF-β1, and TGF-β1 treatment reduced HEL cell proliferation, which is in agreement with a previous study by Catani *et al.* [45]. Moreover, HU-S-PBMSC significantly reduced HEL cell division in co-cultivation experiments, which was mediated in part by both ROS and TGF-β1.

Reactive oxygen species have been implicated in the regulation of cell proliferation. Although, in some specific situations, ROS may promote cell proliferation, they can act as cytostatic/cytotoxic agents. In fact, most of the anticancer drugs affect cancer cell proliferation and survival by inducing the generation of elevated ROS levels [43,46]. Both H_2O_2 and its dismutation products $O_2^{\cdot-}$ reduce cancer cell proliferation, which can be avoided by the addition of catalase to cell cultures. Also, it is possible that H_2O_2 form $OH^{\cdot}$ via Fenton reaction, which also affects cell proliferation [46]. Moreover, ROS mediates paclitaxel inhibition of bystander cells proliferation [47]. This effect is mainly mediated by H_2O_2 production, as evidenced by exogenous catalase in the culture medium to abolish the cytotoxic bystander effect. Nevertheless, further analysis is necessary to determine if H_2O_2 specifically mediates the HU-S-PBMSC inhibition of HEL cell bystander proliferation.

Meanwhile, TGF-β1 is a potent regulator of both adaptive and innate immune system [48]. Although, TGF-β1 seems to mediate the inhibition of bystander HEL cells proliferation, we did not go deeper into the molecular mechanisms. Nevertheless, it has been

demonstrated that the activation of TGF-β-Smad3 signaling reduces acute myeloid leukemia cells proliferation by causing cell cycle arrest at G_1 phase [49]. Moreover, TGF-β1 inhibition enhances acute myeloid cell proliferation in co-culture with BM-MSC [50].

Interestingly, ROS and TGF-β1 interplay has been demonstrated. Actually, ROS can upregulate TGF-β1 gene expression, while TGF-β can increase ROS production by impairing mitochondrial function and NOXs induction, mainly mediated by Smad3 signaling [51]. The fact that APO reduced TGF-β1 expression in HU-S-PBMSC supports this statement. Our analysis indicated the implication of both ROS and TGF-β1, and both mediated the inhibition of bystander HEL cell proliferation.

Conversely to the results of this study, previous studies demonstrated that SASP from senescence fibroblast had the potential to promote bystander proliferation and promote tumorigenesis of epithelial cells, which was independent of the induction of senescence phenotype [52]. This supports the idea that senescence may also promote cancer cell proliferation, while in other cases it may reduce cell proliferation. This can be dependent on the bystander cells type, such as epithelial cancer cells or myeloid transformed cells, and on the senescence cell types, such as fibroblast or MSC, as well as on the RS or SIPS senescence types. Moreover, long-term accumulation of senescence cells can promote tumorigenesis, while short-term senescence cells may act as anticancer cells and improve tissue regeneration [53].

Here, we used *JAK2V617F* mutated myeloid cells that in one way might limit our study. Further studies performed with other *JAK2V617F* harboring cells are necessary to fully understand if *JAK2V617F* mutation may confer some sort of sensibility to HU-induced mesenchymal stromal cell senescence. In addition, we performed analysis by using K562 chronic myeloid leukemia cell line (CML). CML is a MPN disorder characterized by *BCR-ABL1* fusion gene [54]. HU-S-PBMSC did not modify cell proliferation assayed by CFSE dilution analysis (data not shown). K562 dissimilar to HEL cells express very low levels of TGF-β type 2 receptor and respond less to the TGF-β effects on cell proliferation [55,56]. Nevertheless, whether HU alteration of MSC functionality may help in therapy of *JAK2V617F* positive MPN is a matter of importance to address in future investigations.

In summary, HU as a DNA replication stress inducer was able to induce a senescence-like phenotype of PBMSC mainly by increasing oxidative stress cell status. Moreover, HU-S-PBMSC displayed the ROS and TGF-β1-dependent inhibition of HEL cells bystander proliferation. Our results may contribute to the understanding of the underlying genotoxic mechanisms of MSC premature senescence induction by chemotherapy agents, as well as those that are involved in the potential inhibition of MPN transformed myeloid cell proliferation by senescent PBMSC.

Material and methods

Reagents

Anti-CDKN2A/p16^{INK4a} antibody (1D7D2A) was obtained from Abcam (Cambridge, UK). Mab anti p21^{Cip1} was provided by DakoCytomation A/S (Glostrup, DK). HU, APO, *N*-Acetyl Cysteine (NAC), CFSE, propidium iodide (PI), Mytomycin C, the free radical initiator AAPH, 2′,7′-dichlorodihydrofluorescein diacetate (DCFDA), RNase A, Hoechst 33342 trihydrochloride, Diamidine-2′-phenylindole dihydrochloride (DAPI), Dimethylthiazol-2-yl-2,5-diphenyltetrazolium bromide (MTT), NSC23766 trihydrochloride (Rac1 inhibitor) selective inhibitor of TBRi SB525334, and mouse anti a-tubulin antibody coupled to horseradish peroxidase were obtained from Sigma–Aldrich (St. Louis, MO, USA). Recombinant Human LAP (TGF-beta 1) Protein, mouse anti-TGF-beta1 antibody and γH2A.X antibody were obtained from R&D System (Minneapolis, MN, USA).

Cell culture

The PB MSC isolation was performed as previously described [57]. Briefly, mononuclear cells were obtained from the PB of healthy donors by density gradient centrifugation on lymphocyte separation media (PAA Laboratories, Linz, Austria). Cells were plated at density of 2×10^5 per square centimeter in cell culture flasks, and cultured with Dulbecco's modified Eagle's medium (Sigma-Aldrich) supplemented with 10% FBS and 100 units per mL Penicillin/Streptomycin (both from PAA Laboratories) in a humidified atmosphere at 37 °C with 5% CO_2. After 2 or 3 weeks, adherent colonies with fibroblast-like cells became visible. Then, cells were detached and cultured in the above-mentioned conditions. Following the first confluence, cells were passaged regularly, and after three passages, a homogenous cell culture was obtained. The obtained PBMSC, upon appropriate cell culture inductions [58], differentiated into osteogenic and adipogenic phenotypes. Human erythroleukemia HEL92.1.7 (HEL) cell line, homozygous for *JAK2V617F* [59], was kindly provided by S. Hermouet (Laboratoired′Hématologie, Centre Hospitalier Universitaire, Université de Nantes, France). HEL cells were cultured in RPMI 1640 (Sigma) supplemented with 10% FBS and 100 $\mu g \cdot mL^{-1}$ penicillin/streptomycin (Sigma) at 37 °C and 5% CO_2 and maintained regularly at a cell density of 2–4 $\times 10^5$ per mL.

PBMSC immunophenotyping

To phenotype cell-surface antigens, third-passage cells were stained with FITC- or phycoetrythrin (PE)-conjugated antibodies specific for the following human antigens: CD90-PE, CD44-PE, CD73, CD11b (Biosource International, Inc., Camarillo, CA, USA) and CD45-FITC (R&D System), CD105-PE (Invitrogen, Carlsbad, CA, USA). Stained cells were analyzed by flow cytometry, using CyFlow CL (Partec, Munster, Germany). For each sample, at least 10 000 events were recorded [57].

Proliferation assay

The proliferation rate of PBMSC was analyzed by MTT assay as described in [57]. Briefly, 10^4 cells/well were seeded in 96 well plates. The following day, HU (0–600 μM) was added and cells were incubated for indicated days. After this period, MTT (Sigma-Aldrich) was added to each well at 0.5 $mg{\cdot}mL^{-1}$ final concentration, and cells were incubated for additional 2 h. Culture medium was discarded and the cell-precipitated formazan crystals were dissolved in Isopropanol: DMSO (3 : 2) and the absorbance was read at 630 nm in a 96 well plate reader. MTT assay in co-culture conditions were performed by determining formazan production in HEL cells, HU PBMSC pretreated for 3 and 6 days or untreated PBMSC alone and in combination with HEL cells. The absorbance of treated or untreated PBMSC were discounted from absorbance of co-cultured cells following the formula: HEL cell absorbance = (PBMSC + HEL absorbance) − PBMSC absorbance, this was performed assuming that HEL cell in co-cultured condition do not affect PBMSC proliferation.

Crystal violet staining

To analyze changes in cell morphology, cell monolayers were washed twice with PBS and fixed with ice cold methanol for 2 min, then a solution of 0.1% crystal violet was added and incubated either for 10 min for nucleus staining or 20 min for cell staining at room temperature. Cells were extensively washed with distilled water and photographed using and inverted light microscopy.

Immunocytochemistry and senescence-associated β-galactosidase analysis

Senescence-associated β-galactosidase activity was detected by using Senescence Cells Histochemical Staining Kit (Sigma-Aldrich) according to manufacturer's recommendation. Briefly, PBMSC were seeded until 50% confluence and treated with indicated concentrations of HU and indicated days. Cells were then fixed and stained for activity. SA-β-gal positive blue-green-stained cells images were photographed under bright-field microscopy. At least five random fields were counted to determine the percentage of β-gal positive cells in each experimental condition.

Immunofluorescence assay

Immunofluorescence (IF) analysis was used to detect $p16^{INK4}$, $p21^{Cip1}$, and γH2A.X foci. Briefly, 10^5 cells were seeded per rounded cover slip in a 24 well plates and allowed to grow until 50% of confluence. After the indicated treatment, cells were fixed with 4% para-formaldehyde in PBS and permeabilized with 0.2% Triton X-100 for 5 min. Cell monolayers were incubated with specific primary antibodies, followed by incubation with corresponding fluorescently labeled secondary antibodies and 1 $μg{\cdot}mL^{-1}$ DAPI. After mounting with DABCO-Mowiol, the samples were examined and photographed using an epifluorescence microscope.

Cell cycle analysis

Cell cycle analysis was performed by staining cells with PI. Cells were fixed in 70% ethanol for 30 min on ice. The ethanol fixed cells were washed with PBS and million cells were suspended in PBS. Afterwards, cells were centrifuged and 50 μL of RNase A solution (100 $μg{\cdot}mL^{-1}$) was added to ensure that only DNA has been stained. A quantity of 400 μL PI solution was directly added, and cells were incubated in PI solution (50 $μg{\cdot}mL^{-1}$) for 30 min in the dark at room temperature. DNA contents were examined using a BD FACS Calibur (BD Bioscience, San Diego, CA, USA). Flow cytometric data were analyzed using MODFIT LT 5 program (Verity Software House, Topsham, ME, USA).

Detection of intracellular ROS

Intracellular accumulation of ROS was estimated using the membrane-permeable fluorescent DCFDA, which is intracellularly converted into a membrane-impermeable, highly fluorescent compound, dichlorofluorescein by intracellular esterase and ROS. For ROS detection, 20×10^4 cells were seeded in 96-well plates (Corning Inc., Corning, NY, USA) under indicated treatments. Then, cell monolayers were washed 3 × with PBS and lysed with 100 μL of 0.1 M NaOH. Cell extracts were transferred to 96 black wells plates (Corning Inc.) and fluorescence was detected with a CHAMELEON tm, 425–104 MULTILABEL COUNTER (Bioscan, Washington, DC, USA).

CFSE staining and dilution CFSE assay

Briefly, 10^6 HEL cells per mL in PBS-0.1% FBS were stained with 1 μM CFSE for 10 min at room temperature. 1 mL of FBS was added to stop staining and incubated by 10 min, then cells were washed three times with PBS

counted and used for proliferation and adhesion assays as is indicated below. For proliferation analysis, CFSE-stained HEL cells were harvested under indicated treatments, fixed with 2% formaldehyde in PBS and CFSE dilution was analyzed, using a BD FACS Calibur (BD Bioscience). The number of cell division as well as the proliferation index were analyzed using FCS EXPRESS 5 software (De Novo Software, Los Angeles, CA, USA). Proliferation index was calculated as the sum of cells in all generations divided by the number of original parent cells; this index is useful for determining antiproliferative effects on a population of cells [60].

For cytotoxic bystander effects, PBMSC were treated with 200 μM HU for 3 days to induce cells senescence. To obtain similar cell numbers at the end of the treatment period, cells under HU were seeded in six well plates in a range of 1.5 : 1 with untreated PBMSC. HU-treated cells were extensively washed with fresh medium to remove HU. Subsequently, 0.3×10^6 CFSE-stained HEL cells (bystander cells) were added over HU-treated and untreated PBMSC monolayers and incubated for 3 days. Changes in stained HEL cell CFSE dilution, determined as the above-mentioned, indicated the bystander effects. CFSE-stained cells in suspension culture were used as control cells. Also, HEL cells just after CFSE staining were treated with Mytomycin C (40 $\mu g \cdot mL^{-1}$) for 30 min and named as zero time cells.

RT-PCR

Two micrograms of total RNA isolated from 10^6 cells were reverse transcribed using Superscript II (Invitrogen). PCRs were performed using One-Step PCR (Invitrogen) with the following settings: 94 °C for 5 min, 26–30 cycles at 94 °C for 45 s, 52–54 °C for 30 s, and 72 °C for 90 s. The primer sets, annealing temperatures, number of cycles, and product size for TGF-β1 (5′GGGACTATCCACCTGCAAGA3′ and 3′CCTCCTTGGCGTAGTAGTCG5′, 239 bp) and GADPH (5′ACCACAGTCCATGCCATCAC3′ and 3′TCC ACCACCCTGTTGCTGTA5′, 452 bp) were previously reported [61]. Amplicons were resolved in 1.5% agarose gel stained with ethidium bromide. The intensity of the bands was quantified using NIH-IMAGE J software (Bethesda, WA, USA).

ELISA TGF-β1 analysis

Secreted TGF-β1 into cell supernatants was quantified by using Human TGF-β1 ELISA Kit (Abcam) following manufacturer's instructions. Briefly, PBMSC were 3 days treated with 200 mM HU in the presence or absence of 100 μM APO. At the end of the incubation period, cell monolayers were 3× washed with PBS and cultivated two extra days with serum-free medium. Conditioned media were collected, centrifuged at 8000 ***g*** and storage at −20 °C till ELISA analysis. Cell monolayers were lysed with RIPA buffer and total protein content were determined to normalize serum-free conditioned medium.

Statistical analysis

Data are presented as mean standard deviation (SEM) of three independent experiments. Comparisons between two groups were performed using Student's *t*-test. *P*-value 0.05 (*) and 0.005 (**) were considered significant.

Acknowledgements

This research was supported by grants from the Serbian Ministry of Education, Science and Technological Development (OI175053) and by Swiss National Science Foundation through Joint research project, SCOPES: IZ73Z0 152420/1. We thank Dr. Soledad Urrutia, CIBQA, Universidad Bernardo O'Higgins. We are also thankful for the support of the visiting professor program of UBO to JFS. Also, we thank Dr. Tatjana Srdic-Rajic, National Cancer Research Center, Belgrade, Serbia, for her support in TGF-β1 quantification.

Conflict of interest

The authors declare no conflict of interest.

Author contributions

SB, DĐ, MD, MK, and TS performed the research; JFS and VČ designed the research; JFS and VČ provided reagents and tools; SB, DĐ, and MK analyzed the data; SB and JFS wrote the manuscript; MR, OMA, and VČ revised the manuscript.

References

1 Singh A & Xu YJ (2016) The cell killing mechanisms of hydroxyurea. *Genes* **7**, E99.
2 Dong CM, Wang XL, Wang GM, Zhang WJ, Zhu L, Gao S, Yang DJ, Qin Y, Liang QJ, Chen YL *et al.* (2014) A stress-induced cellular aging model with postnatal neural stem cells. *Cell Death Dis* **5**, e1116.
3 Petrova NV, Velichko AK, Razin SV & Kantidze OL (2016) Small molecule compounds that induce cellular senescence. *Aging Cell* **15**, 999–1017.
4 Schmitt CA (2003) Senescence, apoptosis and therapy–cutting the lifelines of cancer. *Nat Rev Cancer* **3**, 286–295.
5 Xu L & Li G (2014) Circulating mesenchymal stem cells and their clinical implication. *J Orthop Translat* **2**, 1–7.

6 He Q, Wan C & Li G (2007) Concise review: multipotent mesenchymal stromal cells in blood. *Stem Cells* **25**, 69–77.
7 de Magalhães JP & Passos JF (2018) Stress, cell senescence and organismal ageing. *Mech Ageing Dev* **170**, 2–9.
8 Burton DG & Krizhanovsky V (2014) Physiological and pathological consequences of cellular senescence. *Cell Mol Life Sci* **71**, 4373–4386.
9 Byun HO, Lee YK, Kim JM & Yoon G (2015) From cell senescence to age-related diseases: differential mechanisms of action of senescence-associated secretory phenotypes. *BMB Rep* **48**, 549–558.
10 Brandl A, Meyer M, Bechmann V, Nerlich M & Angele P (2011) Oxidative stress induces senescence in human mesenchymal stem cells. *Exp Cell Res* **317**, 1541–1547.
11 Burova E, Borodkina A, Shatrova A & Nikolsky N (2013) Sublethal oxidative stress induces the premature senescence of human mesenchymal stem cells derived from endometrium. *Oxid Med Cell Longev* **2013**, 1–12.
12 Korovila I, Hugo M, Castro JP, Weber D, Höhn A, Grune T & Jung T (2017) Proteostasis, oxidative stress and aging. *Redox Biol* **13**, 550–567.
13 Sakano K, Oikawa S, Hasegawa K & Kawanishi S (2001) Hydroxyurea induces site-specific DNA damage via formation of hydrogen peroxide and nitric oxide. *Jpn J Cancer Res* **92**, 1166–1174.
14 Tchkonia T, Zhu Y, van Deursen J, Campisi J & Kirkland JL (2013) Cellular senescence and the senescent secretory phenotype: therapeutic opportunities. *J Clin Invest* **123**, 966–972.
15 Sokol K, Tremblay D, Bhalla S, Rampal R & Mascarenhas JO (2018) Implications of mutation profiling in myeloid malignancies-PART 2: myeloproliferative neoplasms and other myeloid malignancies. *Oncology* **32**, e45–e51.
16 Dominici M, Le Blanc K, Mueller I, Slaper-Cortenbach I, Marini F, Krause D, Deans R, Keating A & ProckopDj Horwitz E (2006) Minimal criteria for defining multipotent mesenchymal stromal cells. International Society for Cellular Therapy position statement. *Cytotherapy* **8**, 315–317.
17 Santos JL, Bosquesi PL, Almeida AE, Chin CM & Varanda EA (2011) Mutagenic and genotoxic effect of hydroxyurea. *Int J Biomed Sci* **7**, 263–267.
18 Petrônio MS, Zeraik ML, Fonseca LM & Ximenes VF (2013) Apocynin: chemical and biophysical properties of a NADPH oxidase inhibitor. *Molecules* **18**, 2821–2839.
19 Sadowska AM, Manuel-Y-Keenoy B & De Backer WA (2007) Antioxidant and anti-inflammatory efficacy of NAC in the treatment of COPD: discordant *in vitro* and *in vivo* dose-effects: a review. *PulmPharmacolTher* **20**, 9–22.
20 Skonieczna M, Hejmo T, Poterala-Hejmo A, Cieslar-Pobuda A & Buldak RJ (2017) NADPH oxidases: insights into selected functions and mechanisms of action in cancer and stem cells. *Oxid Med Cell Longev* **2017**, 1–15.
21 Norozi F, Ahmadzadeh A, Shahrabi S, Vosoughi T & Saki N (2016) Mesenchymal stem cells as a double-edged sword in suppression or progression of solid tumor cells. *Tumour Biol* **37**, 11679–11689.
22 Trivanović D, Krstić J, Jauković A, Bugarski D & Santibanez JF (2018) Mesenchymal stromal cell engagement in cancer cell epithelial to mesenchymal transition. *Dev Dyn* **247**, 359–367.
23 Lunyak VV, Amaro-Ortiz A & Gaur M (2017) Mesenchymal stem cells secretory responses: senescence messaging secretome and immunomodulation perspective. *Front Genet* **8**, 220.
24 Yoshida Y, Itoh N, Saito Y, Hayakawa M & Niki E (2004) Application of water-soluble radical initiator, 2,2'-azobis[2-(2-imidazolin-2-yl)propane] dihydrochloride, to a study of oxidative stress. *Free Radic Res* **38**, 375–384.
25 Alvino GM, Collingwood D, Murphy JM, Delrow J, Brewer BJ & Raghuraman MK (2007) Replication in hydroxyurea: it's a matter of time. *Mol Cell Biol* **27**, 6396–6406.
26 Marusyk A, Wheeler LJ, Mathews CK & DeGregori J (2007) p53 mediates senescence-like arrest induced by chronic replicational stress. *Mol Cell Biol* **27**, 5336–5351.
27 Chabner B (2001) Cancer Chemotherapy and Biotherapy: Principles and Practice, 3rd edn. Lippincott Williams and Wilkins, Philadelphia, PN.
28 Kühr T, Burgstaller S, Apfelbeck U, Linkesch W, Seewann H, Fridrik M, Michlmayr G, Krieger O, Lutz D, Lin W *et al.* (2003) A randomized study comparing interferon (IFN alpha) plus low-dose cytarabine and interferon plus hydroxyurea (HU) in early chronic-phase chronic myeloid leukemia (CML). *Leuk Res* **27**, 405–411.
29 Linke SP, Clarkin KC, Di Leonardo A, Tsou A & Wahl GM (1996) A reversible, p53-dependent G0/G1 cell cycle arrest induced by ribonucleotide depletion in the absence of detectable DNA damage. *Genes Dev* **10**, 934–947.
30 Gottifredi V, Shieh S, Taya Y & Prives C (2001) p53 accumulates but is functionally impaired when DNA synthesis is blocked. *Proc Natl Acad Sci USA* **98**, 1036–1041.
31 Borel F, Lacroix FB & Margolis RL (2002) Prolonged arrest of mammalian cells at the G1/S boundary results in permanent S phase stasis. *J Cell Sci* **115**, 2829–2838.
32 Borodkina A, Shatrova A, Abushik P, Nikolsky N & Burova E (2014) Interaction between ROS dependent

DNA damage, mitochondria and p38 MAPK underlies senescence of human adult stem cells. *Aging* **6**, 481–495.
33 Ziegler-Skilkakis K, Schwarz LR & Andrae U (1985) Microsome- and hepatocyte-mediated mutagenicity of hydroxyurea and related aliphatic hydroxamic acids in V79 Chinese hamster cells. *Mutat Res* **152**, 225–231.
34 Stefanska J & Pawliczak R (2008) Apocynin: molecular aptitudes. *Mediators Inflamm* **2008**, 1–10.
35 Altenhöfer S, Radermacher KA, Kleikers PW, Wingler K & Schmidt HH (2015) Evolution of NADPH oxidase inhibitors: selectivity and mechanisms for target engagement. *Antioxid Redox Signal* **23**, 406–427.
36 Sun J, Ming L, Shang F, Shen L, Chen J & Jin Y (2015) Apocynin suppression of NADPH oxidase reverses the aging process in mesenchymal stem cells to promote osteogenesis and increase bone mass. *Sci Rep* **5**, 18572. https://doi.org/10.1038/srep18572.
37 Yu X, Wang P, Shi Z, Dong K, Feng P, Wang H & Wang X (2015) Urotensin-II-mediated reactive oxygen species generation via NADPH oxidase pathway contributes to hepatic oval cell proliferation. *PLoS ONE* **10**, e0144433.
38 Park JI, Jeong JS, Han JY, Kim DI, Gao YH, Park SC, Rodgers GP & Kim IH (2000) Hydroxyurea induces a senescence-like change of K562 human erythroleukemia cell. *J Cancer Res ClinOncol* **126**, 455–460.
39 Hong SH, Hong B, Kim DC, Rho MS, Park JI, Rha SH, Jun HS & Jeong JS (2004) Involvement of mitogen-activated protein kinases and p21Waf1 in hydroxyurea-induced G1 arrest and senescence of McA-RH7777 rat hepatoma cell line. *ExpMol Med* **36**, 493–498.
40 Narath R, Ambros IM, Kowalska A, Bozsaky E, Boukamp P & Ambros PF (2007) Induction of senescence in MYCN amplified neuroblastoma cell lines by hydroxyurea. *Genes Chromosom Cancer* **46**, 130–142.
41 Yeo EJ, Hwang YC, Kang CM, Kim IH, Kim DI, Parka JS, Choy HE, Park WY & Park SC (2000) Senescence-like changes induced by hydroxyurea in human diploid fibroblasts. *ExpGerontol* **35**, 553–571.
42 Zhai Y, Wei R, Liu J, Wang H, Cai W, Zhao M, Hu Y, Wang S, Yang T, Liu X *et al.* (2017) Drug-induced premature senescence model in human dental follicle stem cells. *Oncotarget* **8**, 7276–7293.
43 Sawal HA, Asghar K, Bureik M & Jalal N (2017) Bystander signaling via oxidative metabolism. *Onco Targets Ther* **10**, 3925–3940.
44 Kobayashi SS, Vali S, Kumar A, Singh N, Abbasi T & Sayeski PP (2016) Identification of myeloproliferative neoplasm drug agents via predictive simulation modeling: assessing responsiveness with micro-environment derived cytokines. *Oncotarget* **7**, 35989–36001.
45 Catani L, Amabile M, Luatti S, Valdrè L, Vianelli N, Martinelli G & Tura S (2001) Interleukin-4 downregulates nuclear factor-erythroid 2 (NF-E2) expression in primary megakaryocytes and in megakaryoblastic cell lines. *Stem Cells* **19**, 339–347.
46 Laurent A, Nicco C, Chéreau C, Goulvestre C, Alexandre J, Alves A, Lévy E, Goldwasser F, Panis Y, Soubrane O *et al.* (2005) Controlling tumor growth by modulating endogenous production of reactive oxygen species. *Cancer Res* **65**, 948–956.
47 Alexandre J, Hu Y, Lu W, Pelicano H & Huang P (2007) Novel action of paclitaxel against cancer cells: bystander effect mediated by reactive oxygen species. *Cancer Res* **67**, 3512–3517.
48 Tu E, Chia PZ & Chen W (2014) TGFβ in T cell biology and tumor immunity: Angel or devil? *Cytokine Growth Factor Rev* **25**, 423–435.
49 Chen J, Mu Q, Li X, Yin X, Yu M, Jin J, Li C, Zhou Y, Zhou J, Suo S *et al.* (2017) Homoharringtonine targets Smad3 and TGF-β pathway to inhibit the proliferation of acute myeloid leukemia cells. *Oncotarget* **8**, 40318–40326.
50 Schelker RC, Iberl S, Müller G, Hart C, Herr W & Grassinger J (2018) TGF-β1 and CXCL12 modulate proliferation and chemotherapy sensitivity of acute myeloid leukemia cells co-cultured with multipotent mesenchymal stromal cells. *Hematology* **23**, 337–345.
51 Liu RM & Desai LP (2015) Reciprocal regulation of TGF-β and reactive oxygen species: a perverse cycle for fibrosis. *Redox Biol* **6**, 565–577.
52 Krtolica A, Parrinello S, Lockett S, Desprez PY & Campisi J (2001) Senescent fibroblasts promote epithelial cell growth and tumorigenesis: a link between cancer and aging. *Proc Natl Acad Sci USA* **98**, 12072–12077.
53 Matjusaitis M, Chin G, Sarnoski EA & Stolzing A (2016) Biomarkers to identify and isolate senescent cells. *Ageing Res Rev* **29**, 1–12.
54 Mughal TI, Abdel-Wahab O, Rampal R, Mesa R, Koschmieder S, Levine R, Hehlmann R, Saglio G, Barbui T & Van Etten RA (2016) Contemporary insights into the pathogenesis and treatment of chronic myeloproliferative neoplasms. *Leuk Lymphoma* **57**, 1517–1526.
55 Wu Y, Su M, Zhang S, Cheng Y, Liao XY, Lin BY & Chen YZ (2017) Abnormal expression of TGF-beta type II receptor isoforms contributes to acute myeloid leukemia. *Oncotarget*. **8**, 10037–10049.
56 Marone M, Scambia G, Bonanno G, Rutella S, de Ritis D, Guidi F, Leone G & Pierelli L (2002) Transforming growth factor-beta1 transcriptionally activates CD34 and prevents induced differentiation of TF-1 cells in the absence of any cell-cycle effects. *Leukemia* **16**, 94–105.
57 Krstić J, Obradović H, Jauković A, Okić-Đorđević I, Trivanović D, Kukolj T, Mojsilović S, Ilić V,

Santibañez JF & Bugarski D (2015) Urokinase type plasminogen activator mediates Interleukin-17-induced peripheral blood mesenchymal stem cell motility and transendothelial migration. *Biochim Biophys Acta* **1853**, 431–444.

58 Toriumi T, Takayama N, Murakami M, Sato M, Yuguchi M, Yamazaki Y, Eto K, Otsu M, Nakauchi H, Shirakawa T *et al.* (2015) Characterization of mesenchymal progenitor cells in the crown and root pulp of primary teeth. *Biomed Res* **36**, 31–45.

59 Martin P & Papayannopoulou T (1982) HEL cells: a new human erythroleukemia cell line with spontaneous and induced globin expression. *Science* **216**, 1233–1235.

60 Roederer M (2011) Interpretation of cellular proliferation data: avoid the panglossian. *Cytometry A* **79**, 95–101.

61 Trivanović D, Jauković A, Krstić J, Nikolić S, Okić-Djordjević I, Kukolj T, Obradović H, Mojsilović S, Ilić V, Santibanez JF *et al.* (2016) Inflammatory cytokines prime adipose tissue mesenchymal stem cells to enhance malignancy of MCF-7 breast cancer cells via transforming growth factor-β1. *IUBMB Life* **68**, 190–200.